ChemComm

Photodoping-based broadband photochromism of semiconductor nanocrystals under air operated by a supramolecular gel

Journal:	*ChemComm*
Manuscript ID	CC-COM-04-2024-001854.R1
Article Type:	Communication

ChemComm

COMMUNICATION

Photodoping-based broadband photochromism of semiconductor nanocrystals under air operated by a supramolecular gel

Received 00th January 20xx,
Accepted 00th January 20xx

DOI: 10.1039/x0xx00000x

Yuki Nakai,[a] Yuki Nagai,*[a] Yoshinori Okayasu [a] and Yoichi Kobayashi *[a]

We herein report photodoping and thereby photochromism of semiconductor nanocrystals under air in a temperature-responsive supramolecular gel and its back reactions induced by direct heating or near-infrared photothermal conversion. We also present their application to the spatiotemporal patterning of photoluminescence.

Inorganic semiconductor nanocrystals (NCs) have been attractive in a wide variety of disciplines, because of the quantum confinement effects, their large specific surface area, and the feasibility of low-cost mass synthesis.[1,2] Photoinduced electron doping (photodoping) of such NCs, resulting from trapping photogenerated holes in the valence band (VB) by hole scavengers,[3,4] enables facile modulation of physical properties of the NCs.[3] In addition, the photodoped electrons in the conduction band (CB) promote Auger recombination to quench photoluminescence from NCs.[5,6] The accumulated free electrons also cause localized surface plasmon resonance (LSPR) and therefore a broad absorption band from the visible to near-infrared (NIR) region. The photogenerated LSPR absorption allows broadband photochromism,[7,8] which is promising for applications like smart windows, whereas such broad absorption changes are difficult to achieve in organic photochromic compounds. The unique characteristics of photodoping have also been applied to various fields other than photochromism, including photocatalysis[9–12] and solar energy storage.[13] However, in general, photodoping occurs only under inert atmospheres because the accumulated electrons react with oxygen, posing large impediments to its wide applications.

As reaction media for achieving oxygen-sensitive photofunctions in aerated conditions, supramolecular gels have attracted much attention, because they suppress molecular and convective diffusion of oxygen.[14–16] In addition, many supramolecular gels display the sol-gel transition upon external stimuli such as temperature and pH changes and light,[17] enabling on-demand oxygen supply from the air. Taking these advantages, we have recently reported reversible photochromism of anthraquinone in a supramolecular gel;[18] photoinduced coloration occurs in the gel state, while heating induces the gel-to-sol transition to cause on-demand decoloration. We have also demonstrated spatiotemporal photochromic patterning based on dissolved oxygen patterning in the gel. Therefore, supramolecular gels are promising for on-demand control under air and enhanced functionalization of photodoping.

In this study, we successfully controlled photodoping and thereby broadband photochromism of TiO_2 and ZnO NCs under air based on on-demand oxygen supply using the sol-gel transition of temperature-responsive supramolecular gel (Fig. 1a), which was prepared by adding a gelator[19] to toluene solution of oleylamine-capped TiO_2 or ZnO NCs, ethanol as a hole scavenger, and oleylamine as an NC-stabilizing reagent (Fig. 1b). In the semi-solid gel state, because oxygen transfer from the air via convective diffusion was suppressed, photodoping occurred under UV light to cause coloration in the visible and NIR region based on LSPR, and the coloration remained for a long time. On the other hand, after the gel-to-sol transition induced by mild heating, oxygen easily permeated the sample and reacted with the accumulated electrons, returning the NCs to the colorless undoped state. Furthermore, LSPR absorption in the photodoped NCs allowed NIR-induced decoloration based on photothermal conversion. UV light irradiation to ZnO NCs in the air-saturated gel also resulted in photodoping-based emission quenching, along with an induction period. We also demonstrated its spatiotemporal patterning for applications to encryption technology.

Oleylamine-capped TiO_2 NCs (average diameter: ~5.1 nm) and the gelator were added into toluene containing oleylamine

[a] *Department of Applied Chemistry, College of Life Sciences, Ritsumeikan University, Kusatsu, Shiga 525-8577, Japan.*
E-mail: ynagai@fc.ritsumei.ac.jp; ykobayas@fc.ritsumei.ac.jp.

† Electronic Supplementary Information (ESI) available: [details of any supplementary information available should be included here]. See DOI: 10.1039/x0xx00000x

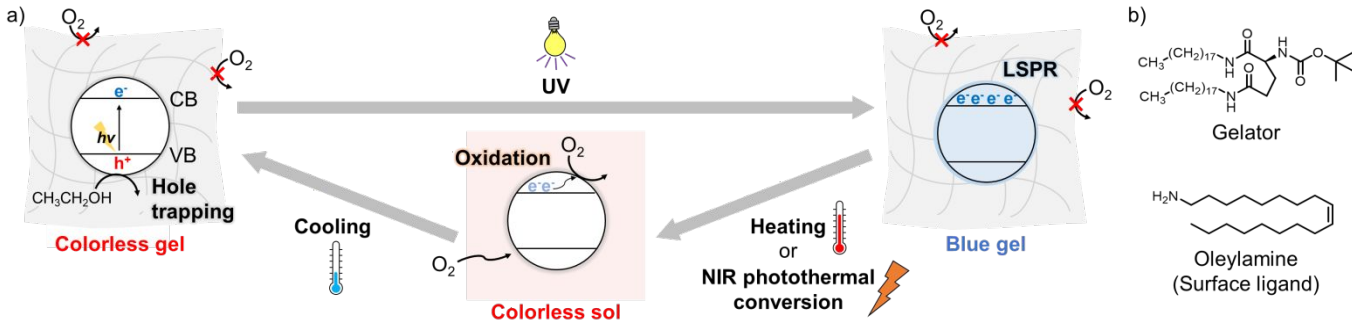

Fig. 1 a) Schematic image of controlling photodoping of semiconductor NCs in temperature-responsive supramolecular gel. b) Molecular structures of the gelator and oleylamine.

and ethanol (several weight percents, respectively), and heated at ~50 °C. Subsequent cooling at room temperature gave TiO_2 NC gel. The formation of supramolecular fibers was observed with scanning electron microscopy (Fig. S6). The as-prepared air-saturated TiO_2 NC gel was slightly yellow-colored (Fig. 2a), because of an absorption tail of the TiO_2 NCs emphasized by the high NC concentration (Fig. 2b red, S4, S5, ESI). 365-nm light irradiation caused a drastic color change to blue despite under the air atmosphere, resulting from the appearance of broad absorption bands in the visible to NIR range (Fig. 2b blue). The coloration origin is ascribed mainly to the LSPR of free electrons in the CB, and some absorption caused by photogenerated Ti^{3+} sites would be overlapping in the visible region (Fig. S8, ESI).[7] Free electron accumulation was also corroborated by a blue shift of the absorption edge, indicating an apparent bandgap increase (the Burstein-Moss effect).[7,20] Heating the colored gel at ~50 °C induced the gel-to-sol transition (the transition temperature $T_{gel\text{-}to\text{-}sol} \approx 35$ °C) and decoloration (Fig. 2b orange). The absorption spectrum after re-gelation by cooling at room temperature was almost consistent with that of the gel before UV light irradiation. Therefore, it suggests that the trapping of the accumulated free electrons (and oxidation of the Ti^{3+} sites)[7] was caused by molecular oxygen penetrating the sol from the air, leading to the decoloration. These results show that supramolecular gels are effective for the reversible control of photodoping under air.

Coloration dynamics of the air-saturated and N_2-purged TiO_2 NC gels were traced under 365-nm light (Fig. 2c). Coloration began to proceed just after starting the photoirradiation in the N_2-purged gel, whereas an induction period for ~100 s before coloration in the air-saturated gel. During the induction period, the dissolved oxygen would be consumed probably via the formation of superoxide anion and subsequent radical chain reactions; for example, a relatively rapid reaction between superoxide anion and ethanol[21] would produce extremely reactive hydroperoxyl radical, leading to reactions with solvents and oleylamine. Notably, the final coloration amount was not sensitive to the originally dissolved oxygen. In addition, decoloration dynamics after 365-nm light irradiation were compared between in the gel state and in the solution without the gelator (Fig. S9, ESI). In the solution, the color started to fade with some fluctuation owing to oxygen permeation via molecular and convective diffusion, and completely disappeared within 4500 s. In contrast, the coloration was maintained to over 90% for 2 hours at least in the gel state because of the oxygen blocking via suppression of convective diffusion (and also possibly molecular diffusion).

Furthermore, the intense NIR absorption of the photodoped TiO_2 NCs motivated us to conduct photothermally induced gel-to-sol transition. Continuous-wave NIR laser irradiation (975 nm, 500 mW) to the photodoped gel caused the gel-to-sol transition and thereby decoloration (Fig. 3a, a movie in ESI). To reveal the decoloration dynamics in detail, temperature and absorption changes were traced at the same time under the NIR laser (Fig. 3b). We note that there was some delay between the temperature and absorption changes because the probe positions were not the same (Figure S10, ESI). NIR laser irradiation brought a temperature rise of 13.9 °C, and the maximum temperature was 38.2 °C, beyond the $T_{gel\text{-}to\text{-}sol}$ (~35 °C). The temperature rise induced the gel-to-sol transition, and oxygen permeation from the air to cause the color fading. The decoloration suppressed the photothermal conversion, and therefore the temperature almost returned to the initial temperature. A negligible temperature change in the un-photodoped gel under the NIR laser also supported that the main origin of the photothermal conversion was photodoping (Fig. S11, ESI). The photothermally induced decoloration is a synergetic effect of photodoping and supramolecular gel. In other words, as well as the temperature-responsive supramolecular gel improves the air-tolerance of photodoping,

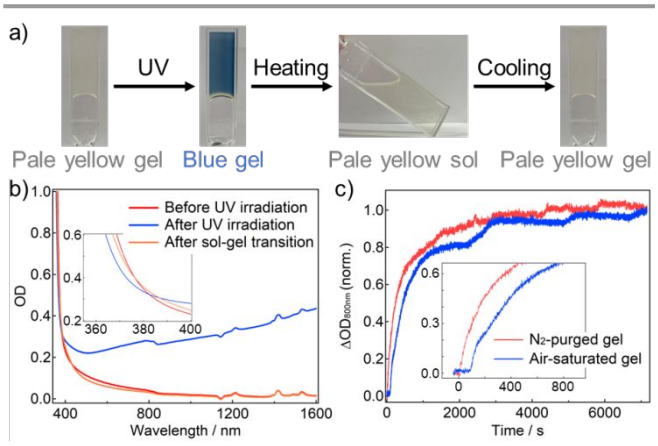

Fig. 2 (a) Sample images of the TiO_2 NC gel (9.7wt% TiO_2 NCs, 2-mm cuvette) upon UV irradiation and the sol-gel transition. (b) Absorption spectra of the TiO_2 NC gel (1.4wt% TiO_2 NCs, 2-mm cuvette) before and after UV light irradiation (365 nm, 105 mW cm^{-2}) and the sol-gel transition. (c) Coloration dynamics at 800 nm in the air-saturated and N_2-purged TiO_2 NC gels (1-mm cuvette) upon UV light irradiation (365 nm, 49 mW cm^{-2}).

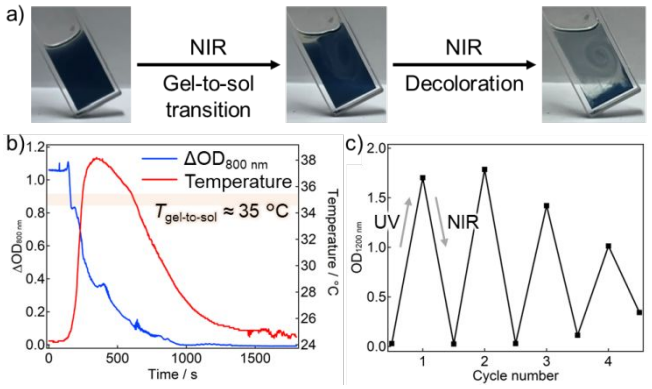

Fig. 3 (a) Sample images of the TiO_2 NCs gel (10wt% TiO_2 NCs, 2-mm cuvette) under NIR laser irradiation. (b) Temperature and absorption (at 800 nm) changes in the TiO_2 NCs gel (10wt% TiO_2 NCs, 2-mm cuvette) under NIR laser (975 nm, 500 mW) irradiation. (c) Repeatability of the UV light-induced coloration and NIR laser-induced decoloration in the TiO_2 NC gel.

its sol-gel transition can be controlled based on the photodoping, which achieves the NIR responsivity of photodoping-based photochromism. In addition, the cyclability of UV-light-induced coloration and NIR-laser-induced decoloration was evaluated (Fig. 3c). The color changes could be repeated four times at least, although some deterioration was caused by formation of precipitates, probably owing to the surface ligand decomposition triggered by hole trapping and/or photochemical superoxide generation.

The results in the TiO_2 NC gel moved us to ZnO NCs, another typical semiconductor NCs showing photodoping. ZnO NC gel was obtained using oleylamine-capped ZnO NCs (average diameter: ~5.6 nm) in the same method as TiO_2 NC gel. Similarly to the TiO_2 NCs, photodoping of the ZnO NCs also proceeded under air by using supramolecular gel; 365-nm light irradiation gave a wide-range absorption band from the visible to NIR region based on LSPR and a blue shift of the band-edge absorption (Fig. S14a,b, ESI). The absorption spectrum reverted to the initial state after the thermally induced gel-sol-gel transition. The decoloration was also induced by the NIR laser (Fig. S15, ESI). These results indicate that using supramolecular gels is widely available for controlling photodoping of semiconductor NCs in the air atmosphere.

Emission properties of the ZnO NCs were also investigated because the NCs displayed yellow emission under UV light (Fig. 4a). The as-synthesized ZnO NCs in toluene exhibited a broad emission band at ~575 nm, attributed to emission from surface oxygen defects (Fig. S16 red, ESI).[22] The relative emission quantum yield in the toluene solution was obtained as 3.5×10^{-2} (vs. anthracene in cyclohexane),[23] and the emission intensity decreased to the ~74% upon addition of oleylamine and ethanol as hole scavengers, because of trapping photogenerated holes (Fig. S16 blue, ESI). The air-saturated ZnO NC gel before photodoping also showed an emission similar to that of the solution (Fig. 4b, red). However, continuous 365-nm light irradiation caused almost complete emission quenching (Fig. 4b, blue). This quenching is ascribed to photodoping, because Gamelin *et al.* have reported that excess electrons in the CB of ZnO NCs quench the visible trap-centered emission via Auger recombination.[5] We mention that emission quenching was incomplete quite near the air-gel interface owing to oxygen permeation from the air. Furthermore, the thermally induced gel-sol-gel transition recovered the initial emission spectrum (Fig. 4b, orange). Thus, emission of the ZnO NCs was reversibly controlled based on photodoping using supramolecular gel.

Emission changes at 575 nm of the N_2-purged and air-saturated dilute ZnO NC gels under 365-nm light were also compared. In the N_2-purged gel, the emission was quenched within 3 s owing to the photodoping. By contrast, the emission was continuously observed for ~2000 s in the air-saturated gel, and thereafter quenching occurred. This induction period is interpreted as the duration until the dissolved oxygen was consumed enough, similarly to the absorption change of the TiO_2 NC gel. Interestingly, absorption at 800 nm of the air-saturated gel, which was measured concurrently with the emission, remained almost constant over the measurement (Fig. S17, ESI). These results show that the emission change was more sensitive to the photodoping than the absorption change in the visible region. Therefore, the gel containing dilute ZnO NCs enables dramatic emission changes without detectable absorption changes in the visible region.

Finally, spatiotemporal photopatterning was attempted using photodoping-based emission quenching along with an induction period in the ZnO NC gel (Fig. 5, a movie in ESI). The air-saturated gel (0.3 wt% ZnO NCs) in a 1-mm cuvette was irradiated with 365-nm light through a photomask composed of parts with different transmittances (71% inside the circle, 58% inside the triangle, and 38% inside the square, at 365 nm). In this step, emission quenching did not occur to give no apparent changes, while the dissolved oxygen concentration was patterned according to the intensity of UV light passing through the photomask; the concentrations in the areas under the circle, triangle, and square were in order from the lowest. As a result, further 365-nm light irradiation to the whole gel after removing the photomask brought sequent emission quenching patterns in the order of the circle, triangle, and square. Notably, almost no color changes were observed under white light in the naked

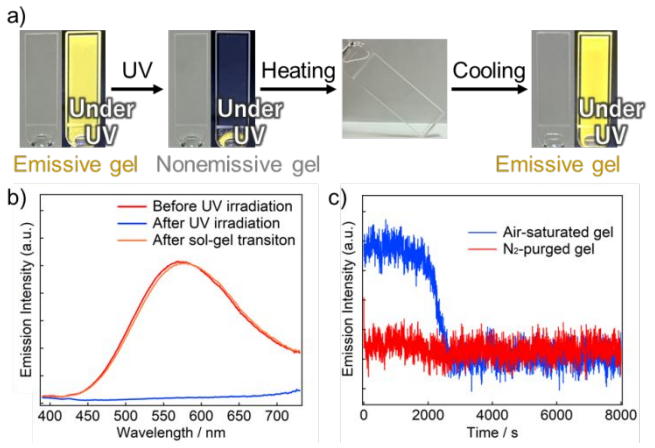

Fig. 4 (a) Sample image of the ZnO NC gel (1.9wt% ZnO NCs, 1-mm cuvette) upon UV irradiation and the sol-gel transition. (b) Emission spectra (λ_{ex}: 380 nm) of the ZnO NC gel (0.4wt% ZnO NCs, 1-cm cuvette) before and after UV light irradiation (365 nm, 25 mW cm^{-2}) and the sol-gel transition. (c) Emission change at 575 nm in the air-saturated and N_2-purged ZnO NC gels (0.02wt% ZnO NCs, 1-cm cuvette) under UV light irradiation (365 nm, 63 mW cm^{-2}).

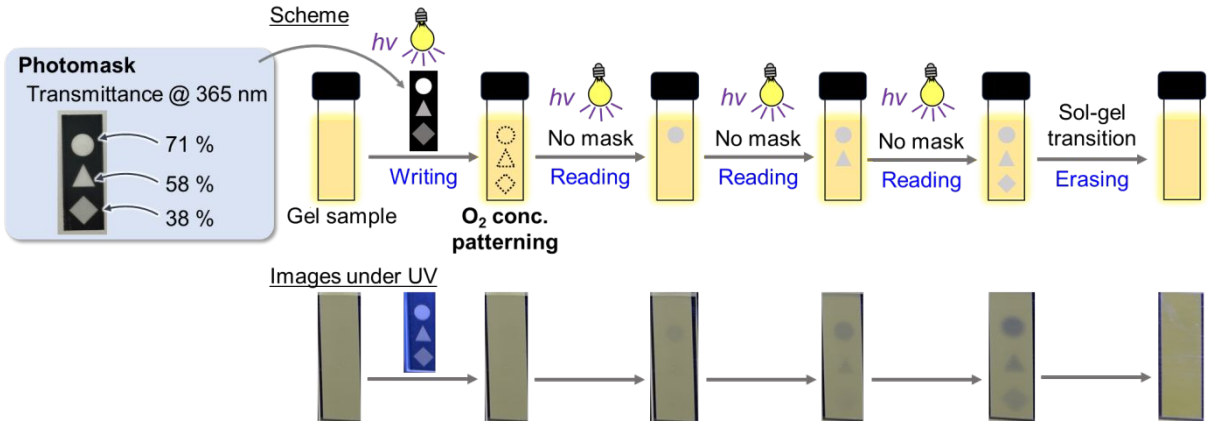

Fig. 5 Spatiotemporal photopatterning experiment using the ZnO NC gel; (top) experimental scheme, (bottom) sample images under UV light (365 nm, 23 mW cm^{-2}).

eye (Fig. S18, ESI). Furthermore, the recorded emission patterns could be erased by the sol-gel transition. As far as we know, this work is the first example of spatiotemporal on-to-off emission patterning, although the off-to-on type has been reported in photoactivated phosphorescence materials.[24,25] Such spatiotemporal emission patterning with little absorption changes is promising for applications to encryption and anticounterfeiting technologies.

In conclusion, we successfully achieved photodoping of TiO_2 and ZnO NCs under air atmosphere using supramolecular gel, giving broadband photochromism from the visible to NIR region. The gel-to-sol transition induced by direct heating or NIR photothermal conversion resulted in the on-demand decoloration. ZnO NCs also exhibited photodoping-based quenching of photoluminescence, along with an induction period owing to the dissolved oxygen. The quenching behavior was applied to spatiotemporal photopatterning. Our strategy provides photodoping not only with availability under air, but also with stimuli-responsivities originating from supramolecular gels, contributing to diverse applications of photodoping as well as photochromism.

This work was supported by JST, PRESTO Grant Numbers JPMJPR22N6, JSPS KAKENHI Grant Numbers JP21K05012, 24K17749, 24K01460, and the Sasakawa Scientific Research Grant from The Japan Science Society.

Conflicts of interest

There are no conflicts to declare.

Notes and references

1 A. M. Smith and S. Nie, *Acc. Chem. Res.*, 2010, **43**, 190–200.
2 N. Pradhan, S. Das Adhikari, A. Nag and D. D. Sarma, *Angew. Chem. Int. Ed.*, 2017, **56**, 7038–7054.
3 A. M. Schimpf, K. E. Knowles, G. M. Carroll and D. R. Gamelin, *Acc. Chem. Res.*, 2015, **48**, 1929–1937.
4 M. Ghini, N. Curreli, A. Camellini, M. Wang, A. Asaithambi and I. Kriegel, *Nanoscale*, 2021, **13**, 8773–8783.
5 A. W. Cohn, N. Janßen, J. M. Mayer and D. R. Gamelin, *J. Phys. Chem. C*, 2012, **116**, 20633–20642.
6 A. W. Cohn, J. D. Rinehart, A. M. Schimpf, A. L. Weaver and D. R. Gamelin, *Nano Lett.*, 2014, **14**, 353–358.
7 U. Joost, A. Šutka, M. Oja, K. Smits, N. Döbelin, A. Loot, M. Järvekülg, M. Hirsimäki, M. Valden and E. Nõmmiste, *Chem. Mater.*, 2018, **30**, 8968–8974.
8 H. Ito, D. Yoshioka, M. Hamada, T. Okamoto, Y. Kobori and Y. Kobayashi, *Photochem. Photobiol. Sci.*, 2022, **21**, 1781–1791.
9 S. O. Obare, T. Ito and G. J. Meyer, *J. Am. Chem. Soc.*, 2006, **128**, 712–713.
10 Y. Li, H. Ji, C. Chen, W. Ma and J. Zhao, *Angew. Chem. Int. Ed.*, 2013, **52**, 12636–12640.
11 G. M. Carroll, A. M. Schimpf, E. Y. Tsui and D. R. Gamelin, *J. Am. Chem. Soc.*, 2015, **137**, 11163–11169.
12 O. Savateev, *Adv. Energy Mater.*, 2022, **12**, 2200352.
13 A. Rogolino and O. Savateev, *Adv. Funct. Mater.*, 2023, **33**, 1–24.
14 P. Duan, N. Yanai, H. Nagatomi and N. Kimizuka, *J. Am. Chem. Soc.*, 2015, **137**, 1887–1894.
15 M. Häring, A. Abramov, K. Okumura, I. Ghosh, B. König, N. Yanai, N. Kimizuka and D. Díaz Díaz, *J. Org. Chem.*, 2018, **83**, 7928–7938.
16 B. Maiti, A. Abramov, R. Pérez-Ruiz and D. Díaz Díaz, *Acc. Chem. Res.*, 2019, **52**, 1865–1876.
17 S. Panja and D. J. Adams, *Chem. Soc. Rev.*, 2021, **50**, 5165–5200.
18 S. Fujisaki, Y. Nagai, Y. Okayasu and Y. Kobayashi, *Mater. Adv.*, 2024, **5**, 1468–1472.
19 Y. Li, T. Wang and M. Liu, *Soft Matter*, 2007, **3**, 1312–1317.
20 I. Hamberg, C. G. Granqvist, K. F. Berggren, B. E. Sernelius and L. Engström, *Phys. Rev. B*, 1984, **30**, 3240–3249.
21 M. Mohammad, A. Y. Khan, M. S. Subhani, N. Bibi, S. Ahmad and S. Saleemi, *Res. Chem. Intermed.*, 2001, **27**, 259–267.
22 Y. Toyota, M. Sagawa, S. Yamashita, Y. Okayasu, Y. Nagai, Y. Okada and Y. Kobayashi, *RSC Adv.*, 2024, **14**, 2796–2803.
23 I. B. Berlman, *Handbook of Fluorescence Spectra of Aromatic Molecules*, Elsevier, 1971.
24 P. She, J. Lu, Y. Qin, F. Li, J. Wei, Y. Ma, W. Wang, S. Liu, W. Huang and Q. Zhao, *Cell Rep. Phys. Sci.*, 2021, **2**, 100505.
25 H. Li, X. Xue, Y. Cao, H. Cheng, A. Luo, N. Guo, H. Li, G. Xie, Y. Tao, R. Chen and W. Huang, *J. Am. Chem. Soc.*, 2023, **145**, 7343–7351.

